B-cell–independent sialylation of IgG

Mark B. Jones[a], Douglas M. Oswald[a], Smita Joshi[b], Sidney W. Whiteheart[b], Ron Orlando[c,d], and Brian A. Cobb[a,1]

[a]Department of Pathology, Case Western Reserve University School of Medicine, Cleveland, OH 44106; [b]Department of Molecular and Cellular Biochemistry, University of Kentucky, Lexington, KY 40536; [c]Complex Carbohydrate Research Center, University of Georgia, Athens, GA 30602; and [d]Department of Biochemistry and Molecular Biology, University of Georgia, Athens, GA 30602

Edited by Laura L. Kiessling, University of Wisconsin-Madison, Madison, WI, and approved May 12, 2016 (received for review December 6, 2015)

IgG carrying terminal α2,6-linked sialic acids added to conserved *N*-glycans within the Fc domain by the sialyltransferase ST6Gal1 accounts for the anti-inflammatory effects of large-dose i.v. Ig (IVIg) in autoimmunity. Here, B-cell–specific ablation of ST6Gal1 in mice revealed that IgG sialylation can occur in the extracellular environment of the bloodstream independently of the B-cell secretory pathway. We also discovered that secreted ST6Gal1 is produced by cells lining central veins in the liver and that IgG sialylation is powered by serum-localized nucleotide sugar donor CMP-sialic acid that is at least partially derived from degranulating platelets. Thus, antibody-secreting cells do not exclusively control the sialylation-dependent anti-inflammatory function of IgG. Rather, IgG sialylation can be regulated by the liver and platelets through the corresponding release of enzyme and sugar donor into the cardiovascular circulation.

IgG | sialylation | sialyltransferase | B cell | IVIg

While en route to the plasma membrane as integral membrane proteins or for secretion, glycoproteins exiting the endoplasmic reticulum traverse the *cis*-, *medial*-, and *trans*-Golgi apparatus where the associated *N*-linked glycans are remodeled into their final form. This classically defined secretory pathway dictates that the glycoform of all glycoproteins produced by a cell is largely determined by the cohort of enzymes within the Golgi and the metabolic circumstances of that specific cell.

Protein glycosylation is known to play fundamental roles in all aspects of biology, but has recently gained significant attention in immunology. When administered at high doses, i.v. Ig (IVIg) is an effective anti-inflammatory treatment for autoimmune patients (1). In 2006, it was discovered that the ∼10% of IgG molecules that carry α2,6-linked sialic acids upon the conserved biantennary *N*-glycans within the Fc domain provided the potent IVIg anti-inflammatory activity in autoimmune disease (2). Indeed, enrichment for the sialylated IgG (sIgG) fraction from IVIg pools increased the efficacy of treatment in mouse models of arthritis 100-fold in an IL-4–dependent fashion through receptors such as CD209 (DC-SIGN) (3, 4). Moreover, it was reported that sialylation of IgG also impacts antibody affinity maturation, although the mechanism underlying this phenomenon remains to be fully elucidated (5). These data indicate that sialylation serves as the mechanism underlying pleotropic IgG function (3, 4, 6).

Epidemiologic analyses published since the reports cited above are consistent with this model. For example, female rheumatoid arthritis patients often go into remission during pregnancy and then relapse following childbirth. Analysis of sIgG levels before, during, and after pregnancy showed that the level of sIgG increases rapidly during pregnancy-induced remission, whereas during periods of exacerbated disease, sIgG is essentially undetectable (7, 8). To date, it is unclear whether IgG sialylation patterns precede or result from the inflammatory state, and essentially nothing is known about the regulatory mechanisms of IgG sialylation within B cells.

Systemically, α2,6-linked sialic acid can be attached to exposed galactose residues only through the action of a single sialyltransferase, ST6Gal1 (9). Germ-line ablation of ST6Gal1 eliminates α2,6-linked sialic acids on IgG and essentially all other glycoproteins in the body (10, 11) with the exception of those in the central nervous system (12). Moreover, modification of the P1 region of the ST6Gal1 promoter generated defects in both myelopoiesis (13) and sialylation of serum glycoproteins (14). Here, we describe the creation of a B-cell–specific knockout of ST6Gal1 that was created to more fully understand the impact of IgG sialylation on autoimmunity. However, analysis of these mice showed normal levels of IgG sialylation. Detailed interrogation of these animals instead revealed that IgG sialylation occurs independently of the secretory pathway in B cells. We discovered that IgG sialylation occurs in the circulation independently of antigen specificity through the action of liver-secreted ST6Gal1, which we found to be powered at least in part by platelet α-granule–derived nucleotide sugar donor CMP-sialic acid (CMP-SA). These findings suggest that B cells do not control the sialylation-dependent activity of IgG molecules, but rather, IgG sialylation is mediated by liver ST6Gal1 and platelet-derived donor within the circulatory system.

Results

B-Cell–Specific Ablation of ST6Gal1. We generated a B-cell–specific conditional knockout (cKO) mouse of the gene encoding ST6Gal1 by crossing animals homozygous for both CD19-CRE and floxed ST6Gal1 alleles with animals lacking CRE but were homozygous for floxed ST6Gal1, leading to F1 progeny with the genotype CD19-CRE$^{+/-}$ST6Gal1$^{fl/fl}$ (*SI Appendix*, Fig. S1*A* and *SI Materials and Methods*). The CD19-CRE locus was maintained as a heterozygote with wild-type CD19 because homozygosity of the CD19-CRE locus ablates CD19 expression, leading to a lack of mature B cells (15). The F1 progeny lack ST6Gal1 in all CD19^{+} B cells, as confirmed by quantitative PCR (qPCR) from magnetically isolated splenic B cells (*SI Appendix*, Fig. S1*B*).

Using the α2,6-linked sialic-acid–specific *Sambucus nigra* lectin (SNA) and terminal galactose-specific *Erythrina cristagalli* lectin (ECL), cell-surface glycan analyses of circulating lymphocytes by flow cytometry revealed a three orders of magnitude loss in α2,6-linked sialic acid and an increase in the amount of terminal galactose on B cells (Fig. 1 *A* and *B*). cKO mice showed an ablation of circulating SNA^{hi}CD19^{+} cells with <2% α2,6 sialic-acid–positive cells compared with 98% found in wild type (Fig. 1*C*) with no effect

Significance

Sialylation of Fc domain glycans on IgG is now a recognized functional switch between pro- and anti-inflammatory antibody function. Creation and analysis of a B-cell–specific knockout of β-galactoside α-2,6-sialyltransferase 1 (ST6Gal1) revealed that IgG sialylation occurs independently of the B-cell secretory pathway and within the bloodstream after IgG secretion. This finding supports a paradigm for exogenous posttranslational modification of glycoproteins that has profound functional significance for IgG functions modulated by the conserved *N*-linked glycan within the Fc domain.

Author contributions: M.B.J. and B.A.C. designed research; M.B.J., D.M.O., S.J., S.W.W., R.O., and B.A.C. performed research; M.B.J., D.M.O., R.O., and B.A.C. analyzed data; and M.B.J., D.M.O., and B.A.C. wrote the paper.

The authors declare no conflict of interest.

This article is a PNAS Direct Submission.

[1]To whom correspondence should be addressed. Email: brian.cobb@case.edu.

This article contains supporting information online at www.pnas.org/lookup/suppl/doi:10.1073/pnas.1523968113/-/DCSupplemental.

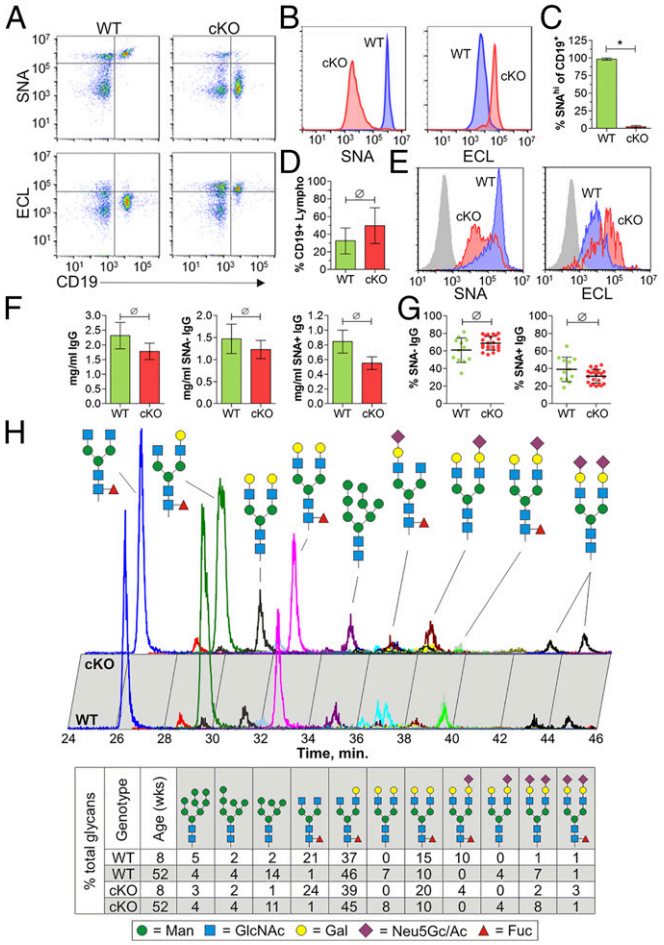

Fig. 1. B-cell–specific, ST6Gal1-deficient cKO mice have normal IgG sialylation. (*A*) Cell-surface glycosylation of circulating lymphocytes was validated using α2,6 sialic-acid–specific (SNA) and terminal galactose-specific (ECL) lectins by flow cytometry with gated CD19$^+$ cell histograms shown in *B* and the percentage of CD19$^+$SNA^{hi} cells in wild-type and cKO mice shown in *C* ($n = 10$). (*D*) Total splenic CD19$^+$ cells were quantified to confirm the lack of a B-cell developmental defect, and (*E*) CD138$^+$B220^{lo} long-lived plasma cell flow cytometry from the bone marrow confirmed that antibody-producing cells were similar to circulating CD19$^+$ B cells in glycosylation. Serum IgG from untreated animals was separated by SNA chromatography and quantified by concentration (*F*) and percentage (*G*) of sialylated IgG from wild type ($n = 12$) compared with cKO ($n = 23$). (*H*) LC-MS analysis of serum IgG glycans from wild-type and cKO animals (*Top*) with the percentage of each glycan calculated and compared for 8- and 52-wk-old animals (*Bottom*). All observed sialic acids in MS structures were α2,6-linked. Mean ± SEM and *P* values are from a two-sided *t* test: *$P < 0.05$, Ø$P > 0.05$.

on the size of the B-cell compartment (Fig. 1*D*). We also analyzed bone marrow resident CD138$^+$CD19$^-$ long-lived plasma cells (LLPCs) for changes in sialylation. Wild-type LLPCs show high SNA and low ECL staining compared with the cKO LLPCs with reduced SNA and increased ECL signals (Fig. 1*E*). These findings are consistent with a B-cell–specific knockout of ST6Gal1.

IgG Sialylation Is B-Cell–Independent. We next quantified the level of total and sialylated IgG by SNA affinity chromatography. Paradoxically, we observed no difference between in IgG titers in wild-type and cKO animals in total, SNA$^-$, and SNA$^+$ IgG fractions (Fig. 1*F*), as well as in the overall degree of IgG sialylation (Fig. 1*G*). Quantitative tandem liquid chromatography–mass spectrometry (LC-MS) confirmed these findings, further showing no difference in the percentage of sIgG between wild-type and cKO animals at either 8 or 52 wk of age (Fig. 1*H*), demonstrating that sIgGs were present throughout the lifetime of the animals. These data demonstrate that B-cell expression of ST6Gal1 is dispensable for the synthesis of sIgG.

IgG Sialylation Is Independent of Antigen Specificity. To discern whether these trends also apply to antigen-specific IgG, mice were immunized and boosted against ovalbumin (OVA) emulsified in Alum. Following the final boost, total (Fig. 2 *A* and *B*) and OVA-specific (Fig. 2 *C* and *D*) IgG were quantified and tested for sialylation. A similar increase in the total amount of circulating IgG was found after immunization with OVA/Alum in both wild-type and cKO animals with no difference in the level of sialylation observed (Fig. 2 *A* and *B*). However, compared with the untreated state, a decrease in the amount of sIgG was seen after sensitization, consistent with previous studies (2, 14). Importantly, the percentage of OVA-specific IgG in both strains was also found to be equivalent (wild type = 6.8 ± 1.12%; cKO = 6.5 ± 1.06%), demonstrating the lack of B-cell defects associated with the loss of ST6Gal1. Finally, we found that OVA-specific sIgG levels were the same or higher in cKO mice compared with their wild-type counterparts (Fig. 2 *C* and *D*).

Cytometric SNA profiling of the CD19$^+$ cells of cKO spleens revealed that a small population (2–13%) remained SNA$^+$ (Figs. 1*A* and 3*E*). These cells are either those that have not yet lost α2,6 sialic acid from the surface following CD19-CRE expression and ST6Gal1 ablation or those that represent a subset of cells that have escaped CRE-lox–mediated recombination. In an effort to ensure that the sIgG is originating from ST6Gal1-ablated B cells, we purified wild-type CD19$^+$SNA^{hi} and cKO CD19$^+$SNA^{lo} populations from OVA-immunized or naive mice by FACS and adoptively transferred them into B-cell–deficient CD19-CRE$^{+/+}$ recipients. The recipients were then immunized against OVA as before. The overall amount of total, SNA$^-$, and SNA$^+$ IgG produced in recipients of cKO donor cells was larger than that in those receiving wild-type cells, possibly due to CD22-mediated hypersensitivity in the absence of *cis* α2,6-sialic acid ligands (16); however, the percentage of SNA$^-$ and SNA$^+$ IgG was indistinguishable (Fig. 3 *A* and *B*). Similar results were found for OVA-specific IgG, including a lack of statistical difference in the amount or percentage of sIgG (Fig. 3 *C* and *D*). Flow analysis of splenic B cells from both groups of B-cell–deficient recipient animals showed populations of CD19$^+$IgD$^+$SNA^{lo} B cells and CD19$^+$IgD$^-$SNA^{lo} memory B cells, confirming equal transfer and expansion of wild-type and

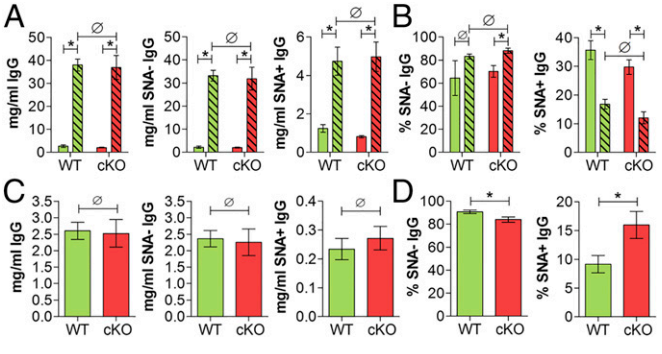

Fig. 2. OVA-specific IgG sialylation in mice with wild-type and ST6Gal1 cKO B cells is indistinguishable. Wild-type and cKO mice were injected i.p. with 50 μg of OVA/Alum and boosted at days 14 and 28 to measure IgG sialylation in response to immunization. Total IgG sialylation by concentration (*A*) or percentage (*B*) from serum of preimmunization (total: wild type, $n = 6$; cKO, $n = 15$) and postimmunization (hatched bars; wild type, $n = 12$; cKO, $n = 18$) was quantified on day 42. The percentage of IgG that was OVA-specific was also quantified (*C*), as was OVA-specific IgG sialylation, shown by concentration (*D*) and percentage of total (*E*). Mean ± SEM and *P* values are two-sided *t* test: *$P < 0.05$, Ø$P > 0.05$.

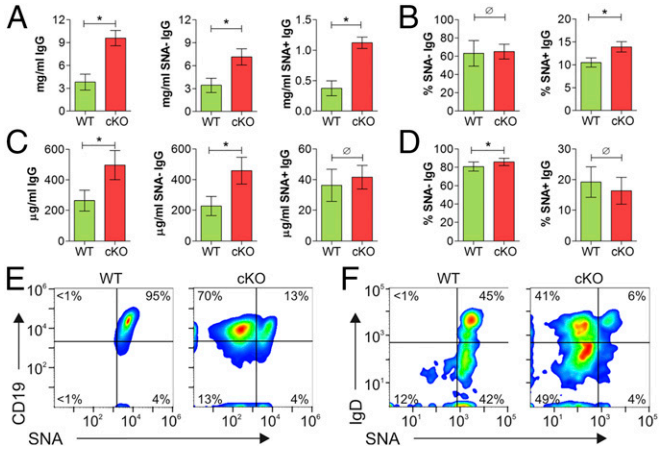

Fig. 3. Adoptive transfer of cKO B cells into B-cell–deficient recipients yields normal IgG sialylation. FACS sorted CD19^{+}SNA^{hi} wild-type or CD19^{+}SNA^{lo} cKO cells from OVA-immunized animals were transferred i.v. into CD19-CRE$^{+/+}$ B-cell–deficient mice. After 24 h, recipients were boosted with OVA/Alum. Total IgG sialylation (wild type, $n = 6$; cKO, $n = 15$) by concentration (*A*) and percentage (*B*) from recipient serum is shown, as is OVA-specific IgG (wild type, $n = 12$; cKO, $n = 18$) by concentration (*C*) and percentage (*D*). (*E*) Flow analysis of B cells (CD19) and sialylation status (SNA) from immunized wild-type and cKO mice before flow sorting and transfer into B-cell–deficient recipients. (*F*) Flow analysis of IgD^{+} memory B-cell sialylation by SNA staining in recipients following immunization. Mean ± SEM and *P* values are two-sided *t* test: **P* < 0.05, Ø*P* > 0.05.

cKO donor cells (Fig. 3*F*). Together, these data reveal that total and antigen-specific IgG produced by sorted ST6Gal1-deficient cells in a B-cell–deficient background is sialylated to normal levels in vivo.

The Liver Cleaves and Secretes ST6Gal1. Enzymatic addition of α2,6 sialic acids to serum-localized glycoproteins such as secreted IgG necessitates the existence of ST6Gal1 in the extracellular environment. ST6Gal1 is already known as a secreted acute phase reactant released ∼72 h after an inflammatory insult (17). In addition, secretion of ST6Gal1 also requires cleavage of its 6-kDa transmembrane domain, which normally anchors the enzyme to the *trans*-Golgi membrane, thereby releasing the active domain into the lumen of the secretory pathway (18, 19). To determine the tissue source of cleaved/secreted ST6Gal1 for IgG sialylation, Western blots were performed from a variety of tissues. We found that the liver was the primary source of cleaved ST6Gal1 (Fig. 4*A*), suggesting that the liver may play a key role in the release of ST6Gal1.

The localization of ST6Gal1 expression and cleavage in the liver was determined using confocal microscopy of wild-type liver sections, staining for ST6Gal1 and its product, α2,6 linked sialic acid, by SNA. We found an organized hierarchy of ST6Gal1 expression in wild-type (Fig. 4*B*) and cKO (*SI Appendix*, Fig. S2*A*) mice in which high and low ST6Gal1 levels correspond to cells surrounding central and portal veins, respectively (Fig. 4*C* and *SI Appendix*, Fig. S2*B*). Cells surrounding central veins also showed a ST6Gal1 signal that increases in intensity with proximity to the vein (Fig. 4*D* and Movie S1) and is characteristic of a delocalized cytoplasmic distribution, almost as if the Golgi apparatus was lost completely. This staining pattern contrasts with the traditional Golgi-associated punctate localization of ST6Gal1 in cells near the portal triad (Fig. 4*E* and Movie S2). Interestingly, the uniform SNA signal throughout the liver tissue demonstrates that the product of ST6Gal1 at the cell surface is decoupled from the intracellular expression level and localization of the enzyme.

Because blood flows through the liver by entering at the portal triad and exiting at the central vein, cleavage and hepatic secretion of ST6Gal1 into the circulation should occur primarily within the tissue surrounding the central veins. To determine whether ST6Gal1 cleavage correlates with central vein proximity, we performed laser capture microdissection on frozen liver tissues within five cells of either central or portal veins (*SI Appendix*, Fig. S3). Captured tissue was either used for quantitative RT-PCR of ST6Gal1 transcript (Fig. 5*A*) or blotted for ST6Gal1 protein (Fig. 5*B*). We found that the cleaved ST6Gal1 was primarily localized to cells near central veins, whereas qRT-PCR revealed a 20-fold increase in ST6Gal1 mRNA expression near the central veins. These data establish preferential ST6Gal1 expression and cleavage by cells lining the central veins, which are ideally localized to release ST6Gal1 into the circulation.

Secreted ST6Gal1 Is Active in the Circulation. Although ST6Gal1 was clearly released into the circulation, we next sought to measure whether it remained a functional sialyltransferase. Sialic acids were removed from mouse serum by mild acid hydrolysis to create substrates for sialylation (20, 21). The asialo-glycoproteins were then separated by SDS/PAGE and transferred to PDVF membranes that were incubated with and without the nucleotide sugar donor CMP-SA and varying amounts of freshly isolated untreated mouse serum or recombinant ST6Gal1 (rST6). Addition of α2,6- and α2,3-linked sialic acid was probed by blotting the membranes with fluorescently conjugated SNA (green) and *Maackia amurensis* lectin I (MAL-I) (red) lectins, respectively. The blots reveal very low levels of α2,3-sialyltransferase activity and high levels of α2,6-sialyltransferase activity that were independent of exogenously added CMP-SA donor (Fig. 6*A*). These findings

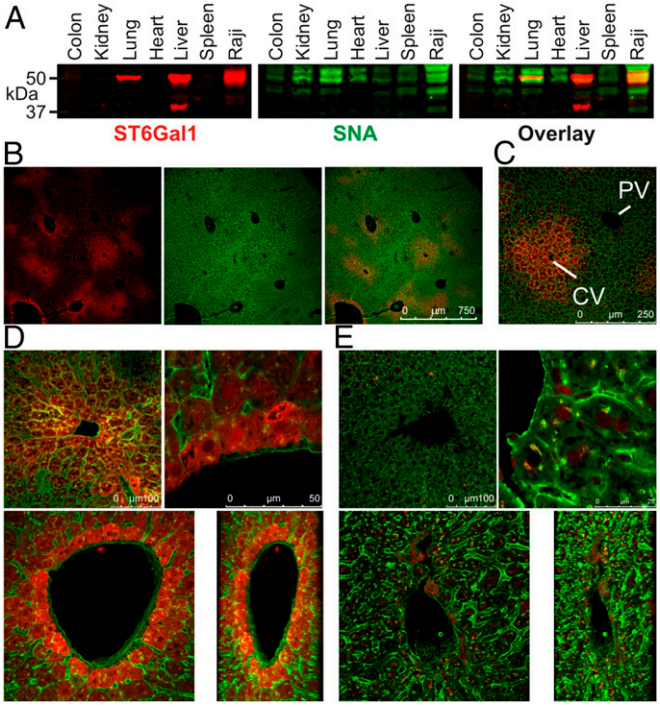

Fig. 4. Secreted ST6Gal1 is predominantly expressed by the liver. (*A*) Total organ lysates were Western-blotted with anti-ST6Gal1 (red; *Left*) and SNA (green; *Middle*) and merged on *Right*. (*B*) Confocal microscopy (10×) of liver sections from untreated wild-type mice stained with anti-ST6Gal1 (red; *Left*) and SNA (green; *Middle* panels) and merged on *Right*. (*C*) A 30± image of a central (CV) and portal (PV) vein. Further magnified images of central (*D*) and portal (*E*) veins demonstrating ST6Gal1 fine localization, including luminal vein wall visualization by 3D reconstruction of *z*-axis stacks (*Bottom Left*) and rotated 45° (*Bottom Right*). Images are representative of at least five mice.

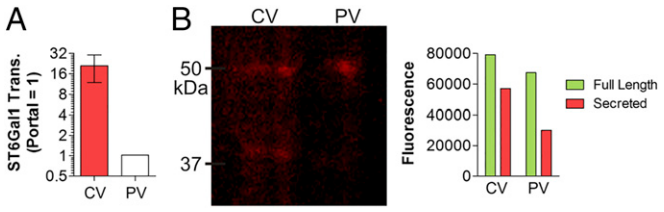

Fig. 5. Secreted ST6Gal1 is concentrated near hepatic central veins. Laser capture microdissected liver tissue from central (CV) and portal (PV) veins was probed for ST6Gal1 mRNA levels by qRT-PCR ($n = 3$) in comparison with GAPDH and normalized to the portal vein (*A*). (*B*) Extracts were also Western-blotted and quantified by fluorescence for ST6Gal1 protein and molecular mass. Mean ± SEM are reported.

demonstrate not only that is ST6Gal1 present and active in serum, but also that mouse serum itself must contain adequate concentrations of CMP-SA to power the transferase reaction.

For a more quantitative approach, we used an ELISA-based activity measurement using the *N*-glycosylated protein fetuin as an immobilized substrate to further quantify the serum-localized activity. As we observed with rST6 (Fig. 6*B*), serum activity adds α2,6-linked sialic acid residues to neuraminidase-treated fetuin, and this activity is inhibited by both CMP and freeze/thaw cycles (Fig. 6*C*), thereby confirming the presence of active ST6Gal1 enzyme and CMP-SA within the serum.

To define the specificity of sialic acid addition by serum-localized enzymatic activity, we tested serum samples for the ability to add α2,6 sialic acids to neuraminidase-treated glycan arrays from the Consortium for Functional Glycomics containing 609 defined glycan targets (*SI Appendix*, Table S1). CMP was also used as a competitive inhibitor of the reaction as a control to ensure that the signal is enzymatically derived. Results from nine representative carbohydrates typically found within *N*-glycans show the addition of α2,6 sialic acids in reactions with either rST6 and CMP-SA donor or serum only (Fig. 6*D*). Sialyltransferase activity was inhibited by CMP, confirming that the signal was based on enzymatic activity, and a comparison between the signals from rST6 and serum revealed a clear Pearson correlation ($r = 0.5173$), suggesting that the serum activity had the same specificity as rST6 (Fig. 6*E*).

Platelets at Least Partially Supply the Nucleotide Sugar Donor. CMP-SA is not believed to be present in the circulation at sufficient concentrations or with appropriate serum lifetime to power sialyltransferase reactions; however, recent studies suggest that platelets release nucleotide sugar donors upon degranulation and lysis (22). Given this controversy, we first performed rST6 enzymatic assays comparing CMP-SA to sialylated glycoprotein donor to confirm that CMP-SA was indeed the source of sialic acid. We found that rST6 is incapable of removing a sialic acid from one glycoprotein and transferring it to another (*SI Appendix*, Fig. S4), as has been reported for the enzyme TS from *Trypanosoma cruzi* (23), thereby ruling out trans-sialidase activity and confirming that CMP-SA is the most likely donor.

We also sought to determine the concentration of CMP-SA within serum. To accomplish this, we freeze/thaw-inactivated serum from two resting wild-type mice to eliminate confounding phosphatase and sialyltransferase activity and then used these inactive samples as a source of CMP-SA in a rST6 enzymatic reaction. Following the reaction, liberated CMP was quantified as previously described for sialyltransferase kinetic studies by coupling the CMP-specific phosphatase CD73 with malachite green detection of free phosphate (24). We found that one sample contained 91 ± 22 μM CMP-SA, whereas another contained 59 ± 27 μM (Fig. 7*A*), yielding an average of 75 μM CMP-SA in serum.

To explore the possibility that platelet activation may contribute to IgG sialylation in the circulation by supplying CMP-SA, we isolated the releasate of thrombin-activated platelets to determine whether it could power rST6 activity. Consistent with previous studies in which 104 pmol of CMP-SA per milligram of platelet granule extract was reported (22, 25), we found that supernatants from activated, but not resting, platelets provided enough CMP-SA to add α2,6-linked sialic acids to target glycans when used in combination with rST6 (Fig. 7*B*). This activity was

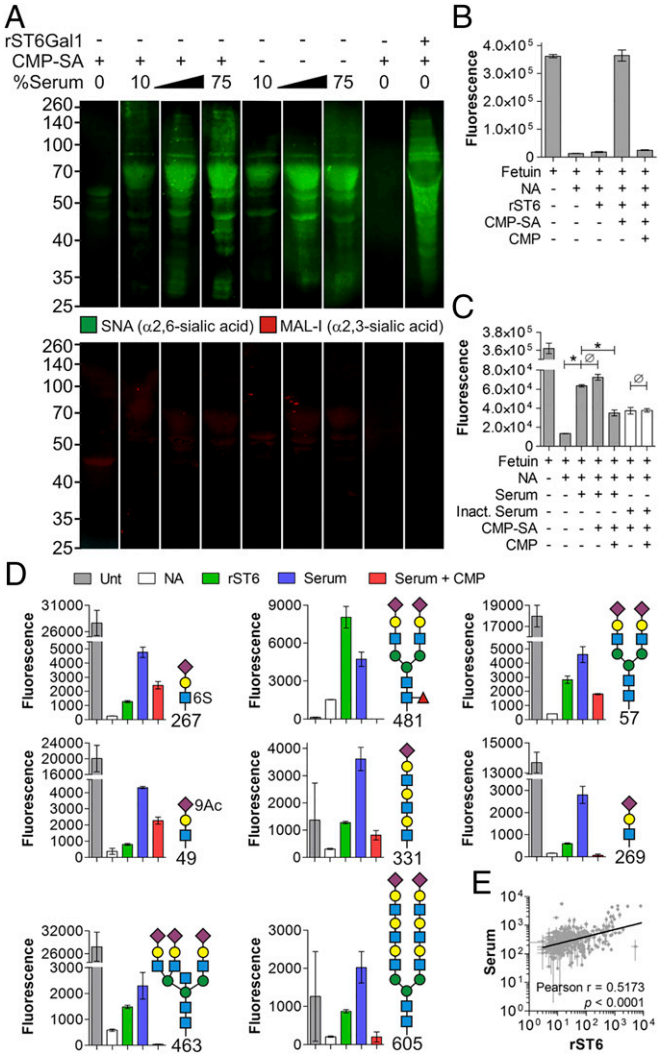

Fig. 6. ST6Gal1 is active in the circulation. (*A*) After removal of sialic acids by mild acid hydrolysis, serum proteins were blotted and incubated with recombinant ST6Gal1 (rST6) or raw serum with and without 100 μM CMP-SA and stained with SNA (green) or MAL-I (red) to quantify α2,6- and α2,3-linked sialic acid products, respectively. (*B*) rST6-mediated sialylation of immobilized and neuraminidase (NA)-treated fetuin and its inhibition by CMP, all quantified by SNA staining ($n = 3$). (*C*) Untreated and heat-inactivated (Inact.) serum-mediated sialylation of immobilized and NA-treated fetuin with and without competitive inhibition by CMP ($n = 3$). (*D*) Untreated (Unt) and NA-treated (NA) glycan array chips from the Consortium for Functional Glycomics were stained with fluorescent SNA as a baseline. NA-treated arrays were incubated with rST6 and CMP-SA (rST6), mouse serum, or serum with CMP as an inhibitor and then quantified with SNA. The top nine glycan targets after serum incubation are shown with the corresponding glycan structures ($n = 2$ arrays with three internal replicates per array). (*E*) Similarity of serum and rST6 specificity were analyzed by Pearson correlation of SNA signals from all array glycans. Mean ± SEM and *P* values are two-sided *t* test: $^*P < 0.05$, $ØP > 0.05$.

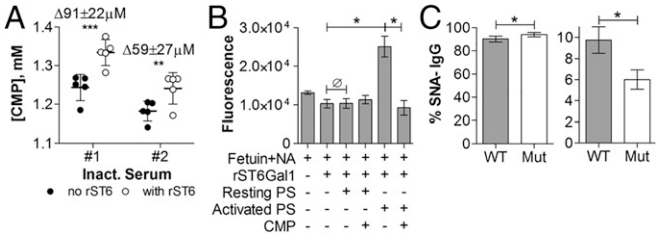

Fig. 7. CMP-SA from platelet granules fuels ST6Gal1 reactions. (*A*) Serum from two independent resting mice was inactivated and then used with rST6 to quantify the concentration CMP-SA within each serum sample by quantifying the liberated CMP following incubation with rST6 as described in *Materials and Methods* ($n = 5$ for each serum; $***P < 0.0008$; $**P < 0.008$). (*B*) rST6 sialylation of immobilized NA-treated fetuin using platelet releaseates as a source of CMP-SA was quantified by adding either resting or thrombin-activated platelet supernatant (PS) at physiological blood volumes with and without CMP inhibition ($n = 3$). (*C*) Percentage of SNA^- and SNA^+ IgG from resting platelet degranulation-deficient $Tomosyn^{-/-}$ (Mut) compared with wild-type controls ($n = 4$). Mean ± SEM and *P* values are two-sided *t* test: $*P < 0.05$, $ØP > 0.05$.

inhibited by the addition of CMP, confirming the enzymatic nature of the signal and further suggesting that platelet activation and degranulation may be an important source of CMP-SA to ST6Gal1 in vivo.

To test this hypothesis, we analyzed the sialylation status of IgG molecules from Tomosyn-$1^{-/-}$ animals, which have normal platelet numbers but an approximately 40% decrease in α-granule release upon activation (26). We found that the Tomosyn-$1^{-/-}$ mice had a concomitant 40% decrease in the percentage of sialylated IgG molecules (Fig. 7*C*), indicating that α-granule release from activated platelets plays an important role in providing CMP-SA for ST6Gal1-mediated IgG sialylation in vivo.

Discussion

The generation of a B-cell–specific knockout of ST6Gal1 suggests that B cells do not control the sialylation-dependent functional switch for IgG described in the context of IVIg-based treatment of autoimmunity (2–4, 6). Rather, our data reveal an entirely different pathway for the remodeling of glycans of secreted, serum-localized glycoproteins: glycoforms of serum proteins are regulated by the release of the enzyme ST6Gal1 from the liver and CMP-SA donor from platelets and possibly other sources. The resulting model enables the immune system to modulate circulatory IgG functionality in a rapid and dynamic fashion that does not rely upon de novo synthesis of IgG.

The initial discovery that IgG α2,6-linked sialylation plays a key role in the suppressive activity of IVIg in autoimmunity was a landmark in the appreciation for the role of glycans in immune responses. Since then, patient studies support the notion that IgG glycosylation directly impacts function. For autoimmunity, terminal galactosylation (27) and terminal sialylation (2–4, 6) are now established factors in immune modulation, whereas fucosylation has been shown to correlate with antibody-dependent cell-mediated viral inhibition (ADCVI) activity in the context of HIV infection (28, 29) as well as antibody-dependent cellular cytotoxicity (ADCC) in vitro (30). For ADCC, structural rearrangements associated with the presence of fucose within the Fc domain appear to account for the functional shift (31), but it remains unclear how fucosylation translates into differential ADCVI activity. Studies focused upon sialylation have revealed that DC-SIGN binds to sIgG, inducing the production of IL-33, which activates basophils to produce IL-4 leading to up-regulation of the inhibitory Fc receptor FcγRIIB (4). In contrast to the ADCVI results that show antigen-specific effects of fucosylation in HIV (29), the sIgG inhibitory activity occurs with isolated Fc domains that lack the antigen-specific Fab fragments, indicating that immune complexes and therefore antigen binding are not required for the suppressive activity (6). This is consistent with our findings that the serum-localized pathway for IgG sialylation appears independently of antigen specificity.

B-cell–independent sialylation also makes teleological sense. In humans, IgG has an average circulatory half-life of about 21 d. Under the established dogma of protein glycosylation, the long half-life would make rapid shifts in the level of IgG sialylation during an inflammatory event or even during inflammation resolution essentially impossible to achieve without a coordinated reprogramming of all antibody-secreted cells and simultaneous removal of existing IgG from the circulation. In contrast, our findings demonstrate the ability to quickly and efficiently sialylate the existing IgG in the circulation through the release of ST6Gal1 into the circulation. Our model, therefore, enables a rapid functional shift in existing IgG that is independent of de novo IgG synthesis and recycling.

A major hurdle to overcome with the notion that any glycosyltransferase, including ST6Gal1, functions within the circulatory environment to remodel glycans on IgG is the source of nucleotide sugar donor required to power the reaction. CMP-SA is the required fuel to power ST6Gal1-mediated additions, yet it has never been found in the circulatory system. In fact, CMP-SA has long been assumed to have a half-life outside of cells that is so short as to preclude its use in enzymatic action, yet the lifetime of extracellular CMP-SA in the rat brain is ∼4 h (32). In our study, we found robust ST6Gal1 activity in serum samples, and this activity did not require the addition of exogenous CMP-SA. Consistent with this observation, we also found an average of 75 μM CMP-SA (range, 59–90 μM) in serum samples from resting mice. Considering that the ST6Gal1 K_m for CMP-SA is 92 μM (33), our findings strongly support a model in which sufficient concentrations of CMP-SA are present in the circulation to power the ST6Gal1 reaction.

Interestingly, studies have revealed that the granules within platelets contain high concentrations of both glycosyltransferase enzymes, although not ST6Gal1 and nucleotide sugar donors, including CMP-SA (22, 25). Indeed, granular concentration of CMP-SA is estimated to be 104 pmol/mg granule extract, suggesting that platelet activation and degranulation could be one source of circulatory CMP-SA. We found that not only did in vitro platelet activation provide a donor for ST6Gal1 activity, but also that mice lacking Tomosyn-1, which show a 40% decrease in α-granule release, have a concomitant 40% reduction in IgG sialylation in vivo. These findings firmly establish a central role for platelets as a key contributor to the B-cell–independent sialylation of IgG by ST6Gal1 in the circulation by providing at least one source of CMP-SA; however, it is likely that other CMP-SA sources exist.

A pathway that extricates the B-cell from IgG functionality is highly significant in itself, yet our findings could impact many other pathways (34). For example, the presence of α2,6-linked sialic-acid–containing glycans is a key regulatory step in B-cell activation through CD22 ligation, thereby setting a key threshold for the differentiation between self-and nonself antigens (35). Another example is the ability of α2,6-linked sialic acid to "cap" glycan structures, reducing the affinity of galectin-1 to its *N*-acetyllactosamine-based ligand. Through differential sialylation, this loss in galectin binding has been linked to T helper cell skewing toward Th2 and Treg and away from Th1 and Th17 lineages (36). In just these two examples, the ability to exogenously modulate the level of α2,6-sialylation represents an unidentified mechanism to prevent or promote autoimmunity or to drive specific T helper phenotypes during activation and differentiation.

Taken to its logical end, extracellular sialylation points to an altered view of systems biology: information from the individual cell and its transcriptome is incomplete outside of its specific and

immediate environmental context. Driven by the release of enzymes by only a few cells, it is now plausible to alter the function of secreted molecules (e.g., cytokines, antibodies) as well as the behavior of other cells in the body. In such a model, it is the collective action of many cells that truly dictates the biological outcome.

Materials and Methods

IgG Quantitation. IgG was enriched from serum by negative selection over Melon Gel (Thermo) and positive selection over SNA-agarose beads (Vector Labs). Unbound IgG (SNA^-) and eluted IgG (SNA^+) were quantified by traditional ELISA titer.

Mass Spectrometry. *N*-linked glycans were released from protein A-purified IgG using PNGaseF, purified, and then derivatized with Procainamide (ProA). Separation of *N*-glycans with sialic acid linkage resolution (37) was conducted with a 2.1-mm i.d. Penta-HILIC column (Advanced Material Technology) coupled in series to an ABI 4000 Q-Trap MS analyzer.

Immunization and Adoptive Transfer. All animals were housed in specific pathogen-free conditions and in accordance with the Institutional Animal Care and Use Committee guidelines at Case Western Reserve University and the University of Kentucky. Mice were immunized i.p. with OVA in Alum (InvivoGen) on days 0, 14, and 28. On day 42, immunized and naive animals were killed, and splenic B cells were purified and i.v.-injected into B-cell–deficient CD19-$CRE^{+/+}$ recipients, which then received OVA/Alum boosters on days 43, 57, and 71 before analysis on day 78.

Laser-Capture Microdissection. Optimal cutting temperature compound (Tissue-Tek) frozen livers were sectioned into 30-μm slices, stained with 50% cresyl violet (Ambion) in ethanol, and laser-dissected with a LMD 7000 system (Leica Microsystems). Laser-cut tissue was captured into Laemmli buffer for Western blots or RNA extraction buffer (mirVana kit, Ambion) for qPCR.

CMP-SA Quantitation. Freeze/thaw-inactivated serum was incubated with and without rST6 in wells containing immobilized asialofetuin. Liberated CMP concentration, and therefore the CMP-SA concentration used, was quantified using a sialyltransferase assay kit as indicated by the manufacturer (R&D Systems).

Statistical Evaluations. For all analyses, two-sided *t* tests between two groups were performed using GraphPad Prism software. Mean ± SEM and associated *P* values at 95% confidence are reported.

See *SI Appendix, SI Materials and Methods* for additional procedures and details.

ACKNOWLEDGMENTS. We thank Patrick Leahy, Jenifer Mikulan, Jenny L. Johnson, and Lori S. C. Kreisman for technical support and Richard D. Cummings and David F. Smith for coordinating the Consortium for Functional Glycomics (CFG) resources. This work was supported by NIH Grants OD004225 and GM082916 (to B.A.C.), AI007024 and AI114109 (to M.B.J.), AI089474 (to D.M.O.), GM062116 and GM098791 to the CFG, and HL056652 (to S.W.W.). Support also came from the Mizutani Foundation for Glycoscience (14-0023) and a Case Western Reserve University Clinical & Translational Science Collaborative Core Utilization Grant 06197 (to B.A.C.).

1. Dwyer JM (1992) Manipulating the immune system with immune globulin. *N Engl J Med* 326(2):107–116.
2. Kaneko Y, Nimmerjahn F, Ravetch JV (2006) Anti-inflammatory activity of immunoglobulin G resulting from Fc sialylation. *Science* 313(5787):670–673.
3. Anthony RM, Wermeling F, Karlsson MC, Ravetch JV (2008) Identification of a receptor required for the anti-inflammatory activity of IVIG. *Proc Natl Acad Sci USA* 105(50):19571–19578.
4. Anthony RM, Kobayashi T, Wermeling F, Ravetch JV (2011) Intravenous gammaglobulin suppresses inflammation through a novel T(H)2 pathway. *Nature* 475(7354): 110–113.
5. Wang TT, et al. (2015) Anti-HA glycoforms drive B cell affinity selection and determine influenza vaccine efficacy. *Cell* 162(1):160–169.
6. Anthony RM, et al. (2008) Recapitulation of IVIG anti-inflammatory activity with a recombinant IgG Fc. *Science* 320(5874):373–376.
7. Espy C, et al. (2011) Sialylation levels of anti-proteinase 3 antibodies are associated with the activity of granulomatosis with polyangiitis (Wegener's). *Arthritis Rheum* 63(7):2105–2115.
8. van de Geijn FE, et al. (2009) Immunoglobulin G galactosylation and sialylation are associated with pregnancy-induced improvement of rheumatoid arthritis and the postpartum flare: Results from a large prospective cohort study. *Arthritis Res Ther* 11(6):R193.
9. Martin LT, Marth JD, Varki A, Varki NM (2002) Genetically altered mice with different sialyltransferase deficiencies show tissue-specific alterations in sialylation and sialic acid 9-O-acetylation. *J Biol Chem* 277(36):32930–32938.
10. Barb AW, Brady EK, Prestegard JH (2009) Branch-specific sialylation of IgG-Fc glycans by ST6Gal-I. *Biochemistry* 48(41):9705–9707.
11. Hennet T, Chui D, Paulson JC, Marth JD (1998) Immune regulation by the ST6Gal sialyltransferase. *Proc Natl Acad Sci USA* 95(8):4504–4509.
12. Lehoux S, et al. (2010) Transcriptional regulation of the human ST6GAL2 gene in cerebral cortex and neuronal cells. *Glycoconj J* 27(1):99–114.
13. Jones MB, et al. (2010) Role for hepatic and circulatory ST6Gal-1 sialyltransferase in regulating myelopoiesis. *J Biol Chem* 285(32):25009–25017.
14. Jones MB, Nasirikenari M, Lugade AA, Thanavala Y, Lau JT (2012) Anti-inflammatory IgG production requires functional P1 promoter in β-galactoside α2,6-sialyltransferase 1 (ST6Gal-1) gene. *J Biol Chem* 287(19):15365–15370.
15. Rickert RC, Roes J, Rajewsky K (1997) B lymphocyte-specific, Cre-mediated mutagenesis in mice. *Nucleic Acids Res* 25(6):1317–1318.
16. Collins BE, Smith BA, Bengtson P, Paulson JC (2006) Ablation of CD22 in ligand-deficient mice restores B cell receptor signaling. *Nat Immunol* 7(2):199–206.
17. Kaplan HA, Woloski BM, Hellman M, Jamieson JC (1983) Studies on the effect of inflammation on rat liver and serum sialyltransferase. Evidence that inflammation causes release of Gal beta 1 leads to 4GlcNAc alpha 2 leads to 6 sialyltransferase from liver. *J Biol Chem* 258(19):11505–11509.
18. Colley KJ, Lee EU, Adler B, Browne JK, Paulson JC (1989) Conversion of a Golgi apparatus sialyltransferase to a secretory protein by replacement of the NH2-terminal signal anchor with a signal peptide. *J Biol Chem* 264(30):17619–17622.
19. Weinstein J, Lee EU, McEntee K, Lai PH, Paulson JC (1987) Primary structure of beta-galactoside alpha 2,6-sialyltransferase. Conversion of membrane-bound enzyme to soluble forms by cleavage of the NH2-terminal signal anchor. *J Biol Chem* 262(36): 17735–17743.
20. Schauer R (1978) Characterization of sialic acids. *Methods Enzymol* 50:64–89.
21. Varki A, Diaz S (1984) The release and purification of sialic acids from glycoconjugates: Methods to minimize the loss and migration of O-acetyl groups. *Anal Biochem* 137(1):236–247.
22. Wandall HH, et al. (2012) The origin and function of platelet glycosyltransferases. *Blood* 120(3):626–635.
23. Colli W (1993) Trans-sialidase: A unique enzyme activity discovered in the protozoan Trypanosoma cruzi. *FASEB J* 7(13):1257–1264.
24. Wu ZL, Ethen CM, Prather B, Machacek M, Jiang W (2011) Universal phosphatase-coupled glycosyltransferase assay. *Glycobiology* 21(6):727–733.
25. Lee MM, et al. (2014) Platelets support extracellular sialylation by supplying the sugar donor substrate. *J Biol Chem* 289(13):8742–8748.
26. Ye S, et al. (2014) Platelet secretion and hemostasis require syntaxin-binding protein STXBP5. *J Clin Invest* 124(10):4517–4528.
27. Karsten CM, et al. (2012) Anti-inflammatory activity of IgG1 mediated by Fc galactosylation and association of FcgammaRIIB and dectin-1. *Nat Med* 18(19): 1401–1406.
28. Ackerman ME, et al. (2013) Enhanced phagocytic activity of HIV-specific antibodies correlates with natural production of immunoglobulins with skewed affinity for FcγR2a and FcγR2b. *J Virol* 87(10):5468–5476.
29. Ackerman ME, et al. (2013) Natural variation in Fc glycosylation of HIV-specific antibodies impacts antiviral activity. *J Clin Invest* 123(5):2183–2192.
30. Shields RL, et al. (2002) Lack of fucose on human IgG1 N-linked oligosaccharide improves binding to human Fcgamma RIII and antibody-dependent cellular toxicity. *J Biol Chem* 277(30):26733–26740.
31. Mizushima T, et al. (2011) Structural basis for improved efficacy of therapeutic antibodies on defucosylation of their Fc glycans. *Genes Cells* 16(11):1071–1080.
32. Ferwerda W, Blok CM, Heijlman J (1981) Turnover of free sialic acid, CMP-sialic acid, and bound sialic acid in rat brain. *J Neurochem* 36(4):1492–1499.
33. Meng L, et al. (2013) Enzymatic basis for N-glycan sialylation: Structure of rat α2,6-sialyltransferase (ST6GAL1) reveals conserved and unique features for glycan sialylation. *J Biol Chem* 288(48):34680–34698.
34. Varki A, Gagneux P (2012) Multifarious roles of sialic acids in immunity. *Ann N Y Acad Sci* 1253:16–36.
35. Macauley MS, et al. (2013) Antigenic liposomes displaying CD22 ligands induce antigen-specific B cell apoptosis. *J Clin Invest* 123(7):3074–3083.
36. Toscano MA, et al. (2007) Differential glycosylation of TH1, TH2 and TH-17 effector cells selectively regulates susceptibility to cell death. *Nat Immunol* 8(8):825–834.
37. Tao S, Huang Y, Boyes BE, Orlando R (2014) Liquid chromatography-selected reaction monitoring (LC-SRM) approach for the separation and quantitation of sialylated N-glycans linkage isomers. *Anal Chem* 86(21):10584–10590.